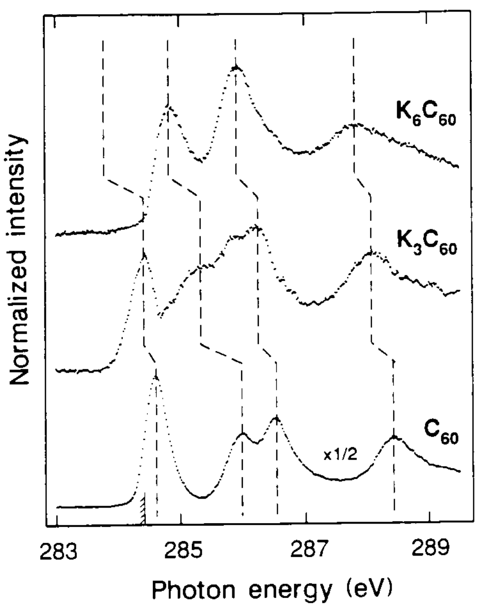

FIG. 4 C 1*s* absorption spectra for the three phases of K_xC_{60}. The shaded vertical line at the bottom indicates the C 1*s* excitation threshold for the superconducting phase.

valence photoemission curves, then this procedure should give the same spectrum for K_3C_{60} in the limits of low and high K concentration. This assumption is justified by internal consistency tests of the absorption data, where all spectra can be fitted by combinations of the three pure-phase spectra, C_{60}, K_3C_{60}, and K_6C_{60}, shown in Fig. 4.

The width of the peak in the K_3C_{60} absorption spectrum at the threshold is due almost entirely to the width of the carbon core level. This sharp peak indicates that there is an edge singularity effect in the excitation spectrum from K_3C_{60}, that is, a metallic exciton. Energy bands of similar character are found to shift toward the excitation threshold in the three phases. The area of the threshold peak in the K_3C_{60} spectrum is exactly half the area of the LUMO in C_{60}. The important observation is that there is not a rigid-band shift of the C_{60} orbitals in these three phases. These observations clearly demonstrate the C 2*p* character of the energy band near ε_F observed in photoemission. Coupled with the anomalous occupied-band width in K_3C_{60}, these results imply a considerable hybridization between the electronic states of K and C_{60} in the superconducting phase. Presumably, this hybridization is responsible for the electron-phonon coupling, which together with the relatively high value of the DOS at ε_F suggests that K_3C_{60} may be a weak-coupling BCS-type superconductor. □

Received 26 June; accepted 26 July 1991.

1. Fujiomori, A., Takayam-Muromachi, E., Uchida, Y. & Okai, B. *Phys. Rev.* **B35,** 8814 (1987).
2. van der Marel, D., van Elp, J., Sawatzky, G. A. & Heitmann, D. *Phys. Rev.* **B37,** 5136 (1988).
3. Shen, Z.-X. *et al. Phys. Rev.* **B36,** 8414 (1987).
4. Chen, C. T. *et al. Phys. Rev. Lett.* **66,** 104 (1991).
5. Hebard, A. F. *et al.* Nature **350,** 600–601 (1991).
6. Rosseinsky, M. J. *et al. Phys. Rev. Lett.* **66,** 2830–2832 (1991).
7. Holczer, K. *et al. Science* **252,** 1154–1157 (1991).
8. Krätschmer, W., Lamb, L. D., Fostiropoulos, K. & Huffman, D. R. *Nature* **347,** 354–358 (1990).
9. Chen, C. T. *Nucl. Instr. Methods* A**256,** 595 (1987).
10. Chen, C. T. & Sette, F. *Rev. Sci. Instrum.* **60,** 1616–1621 (1989).
11. Weaver, J. H. *et al. Phys. Rev. Lett.* **66,** 1741–1744 (1991).
12. Martins, J. L., Troullier, N. & Weaver, J. H. *Chem. Phys. Lett.* **180,** 457–460 (1991).
13. Erwin, S. C. & Pederson, M. R. *Phys. Rev. Lett.* (submitted).
14. Haddon, R. C. *et al. Nature* **350,** 320–322 (1991).
15. Benning, P. J., Martins, J. L., Weaver, J. H., Chibante, L. P. F. & Smalley, R. E. *Science* **252,** 1417–1419 (1991).
16. Wertheim, G. K. *et al. Science* **252,** 1419–1521 (1991).
17. Cheng, A. & Klein, M. L. *Phys. Rev. Lett.* (submitted).
18. Zhou, O. *et al. Nature* **351,** 462–464 (1991).
19. Stephens, P. W. *et al. Nature* **351,** 632–634 (1991).

ACKNOWLEDGEMENTS. We thank E. J. Mele, G. K. Wertheim and J. Zaanen for discussions. This research was partially funded by NSF. The National Synchrotron Light Source is supported by the DOE.

Magnetic-field penetration depth in K_3C_{60} measured by muon spin relaxation

Y. J. Uemura*, A. Keren*, L. P. Le*, G. M. Luke*, B. J. Sternlieb*, W. D. Wu*, J. H. Brewer†, R. L. Whetten‡, S. M. Huang‡, Sophia Lin‡, R. B. Kaner‡, F. Diederich‡, S. Donovan§, G. Grüner§ & K. Holczer§

* Department of Physics, Columbia University, New York, New York 10027, USA
† TRIUMF and Department of Physics, University of British Columbia, Vancouver, British Columbia, V6T 2A3, Canada
‡ Department of Chemistry and Biochemistry, University of California, Los Angeles, California 90024, USA
§ Department of Physics, University of California, Los Angeles, California 90024, USA

THE discovery[1–3] of superconductivity in C_{60} doped with the alkali metals potassium and rubidium has introduced a new family of three-dimensional molecular superconductors[4]. The potassium-doped compound[3] K_3C_{60} has a relatively high transition temperature ($T_c = 19.3$ K), a very high upper critical field ($H_{c2}(T \to 0) \approx 50T$) and a short superconducting coherence length[5] ($\xi = 26$ Å), in common with the copper oxide superconductors. Here we report muon-spin-relaxation measurements of the magnetic-field penetration depth λ in K_3C_{60}. The temperature dependence of λ and of the muon spin relaxation rate indicate that the superconducting energy gap is isotropic, without nodes or zero points. The low-temperature penetration depth $\lambda(T \to 0)$ is about 4,800 Å, which implies a ratio of superconducting carrier density to effective mass to be $n_s/(m^*/m_e) = 1.2 \times 10^{20}$ cm^{-3} if one assumes the 'clean limit'. Combining this result with the value of ξ, we estimate the Fermi temperature $T_F = 470$ K. In the relationship between T_F and T_c, K_3C_{60} conforms to the trend exhibited by 'exotic' superconductors[6,7] such as the Chevrel phase compounds, the copper oxides and the organic BEDT systems.

The muon-spin-relaxation (μSR) technique has been extensively applied in the study of the penetration depth in various type-II superconductors[8–10]. In transverse-field μSR (TF-μSR) measurements of λ, we apply an external magnetic field H_{ext} ($H_{c1} \ll H_{ext} \ll H_{c2}$), and observe the spin precession of positive muons implanted in the specimen. In the superconducting state, the field H_{ext} forms a lattice of flux vortices in the specimen, resulting in a local magnetic field B having a distribution with a width ΔB proportional to λ^{-2}. In the spectra of muon spin precession, the oscillation amplitudes are damped because of the inhomogeneity of the local field B. This damping is usually described by a gaussian envelope $G_x(t) = \exp(-\frac{1}{2}\sigma^2 t^2)$ which defines the muon spin relaxation rate $\sigma \propto \Delta B \propto \lambda^{-2}$.

The specimen of K_3C_{60} was prepared at UCLA following the procedures described in ref. 3. A polycrystalline powder material weighing 135 mg was pressed into a sintered pellet ~1 cm in diameter and 1 mm thick. Before pressing, the powder sample showed a shielding diamagnetism ranging from 40 to 60% of a bulk niobium reference. The difference from the reference is mostly due to the small packing density of the powder. Pressing and sintering results in an onset of bulk (100%) shielding at a temperature ~1 K lower than $T_c = 19.3$ K (ref. 11). X-ray studies on a similar specimen[4], sensitive to microscopic-scale inhomogeneity, set an upper limit of 15% volume fraction for presumably nonsuperconducting minority phases. The sintered specimen for μSR was mounted in a ^{4}He gas flow cryostat with its face normal to the beam direction along which the external field was applied. During the whole procedure of sample preparation and μSR measurements, the specimen was kept under vacuum or in dry He gas, except for an interval of less than 1 minute during its loading into the cryostat. A polarized positive muon beam from the M15 channel of TRIUMF was stopped in the specimen, and the time spectra of muon decay events were recorded with an apparatus described in ref. 10.

We made two sets of measurements with a transverse external field of $H_{ext} = 1$ kG and 2 kG applied perpendicular to the initial muon-spin polarization. Figure 1 shows the precession signal in the time spectra plotted using a rotating reference frame. We observed a long-lived oscillation in H_{ext} above T_c and evident depolarization below T_c on cooling because of the inhomogeneous field distribution in the vortex state. There is only a minimal long-lived precessing component remaining after $t \approx 6$ μs at $T = 3.3$ K. Generally, signals from superconducting and nonsuperconducting regions in the specimen combine additively to give the total μSR signal, with initial precession amplitudes proportional to their volume fractions. The data at $T = 3.3$ K in Fig. 1 indicate that the volume of nonsuperconducting region contributing to the background long-lived signal is less than 10% of the total volume. The present data can be fitted reasonably well with a gaussian curve for $G_x(t)$. After correcting for a small depolarization due to nuclear dipolar fields $\sigma_{nd} = 0.08\ \mu s^{-1}$ observed above T_c, we obtained the flux-lattice-induced relaxation rate σ from the observed relaxation rate σ_{obs} as $\sigma^2 = \sigma^2_{obs} - \sigma^2_{nd}$.

The temperature dependence of the relaxation rate σ is shown in Fig. 2*a*. In the field-cooling (FC) measurements, σ increases with decreasing temperature below T_c, and then saturates at low temperatures. There is essentially no dependence of σ on H_{ext}, as expected from theories[12,13] in which ΔB is due to flux-vortex lattice. Separate zero-field μSR measurements show no effect of static magnetic order, confirming that σ is due purely to superconductivity. The corresponding values of the penetration depth $\lambda(T)$ are shown in Fig. 2*b*. The low-temperature penetration depth $\lambda(T \to 0)$ is ~4,800 Å, with a systematic error due to possible nonsuperconducting volume less than ±200 Å. Note that the value of λ could vary systematically by up to about ±15% depending on different models for field distributions and functional forms of $G_x(t)$. For the conversion factor α in $\lambda = \alpha \times \sigma^{-1/2}$ with λ in Å and σ in μs^{-1}, Pincus *et al.*[12] (after modifying for the triangular lattice) obtained $\alpha = 2,700$. The Brandt model[13] gives $\alpha = 3,270$ if we substitute $\sqrt{M_2}$, where M_2 is the second moment of the field distribution, as σ/γ_μ (γ_μ is the gyromagnetic ratio of μ^+). The 'high-field tail' in the Brandt field distribution, contributing heavily to M_2, is not well represented when we fit $G_x(t)$ with a gaussian shape. Thus the fitted value of σ for the Brandt distribution corresponds to $\sim 0.7\sqrt{M_2} \times \gamma_\mu$, according to our numerical simulations. The Brandt model then also yields $\alpha \approx 2,700$. We use this conversion factor.

The μSR result for λ is somewhat larger than $\lambda(T \to 0) \approx 2,400$ Å estimated from $H_{c1} \approx 130$ G (ref. 5). We note that H_{c1} generally tends to be overestimated because of the effects of flux pinning, yielding underestimates for λ. In contrast, μSR results in field-cooling measurements are not affected by flux pinning. As we discuss later, we found evidence for flux pinning in K_3C_{60} even at temperatures very close to T_c. Another possible source of the difference in the λ values in μSR and H_{c1} studies is the small grain size, typically ~10,000 Å. The closeness of λ to the grain size could significantly affect the H_{c1} results. The approximate vortex separation in the fields $H_{ext} \approx 1$-2 kG used in this μSR study is ~1,000 Å. About 100 vortices exist in a grain, suggesting that the effect of grain size may be less important in μSR than in H_{c1} measurements.

As $\sigma \propto \lambda^{-2}$ is proportional to the density of superconducting carriers n_s which screen the external field, thermal pair-breaking excitations across the energy gap reduce n_s and σ, and λ therefore increases at finite temperatures. This feature allows study of the gap symmetry by μSR. Analysing the observed temperature dependence $\sigma(T)$ with a trial formula $[1-(T/T_c)^\alpha]$, we obtain the best fit for $\alpha = 3.2$ (solid line in Fig. 2*a*) and $T_c = 18.9$ K. This value of α is close to $\alpha = 4$ expected in the two-fluid model[14] for isotropic superconductors. As shown in Fig. 2*b*, the observed results of $\sigma(T)$ lie between the curves for the two-fluid model and for the weak-coupling BCS model[14] for s-wave supercon-

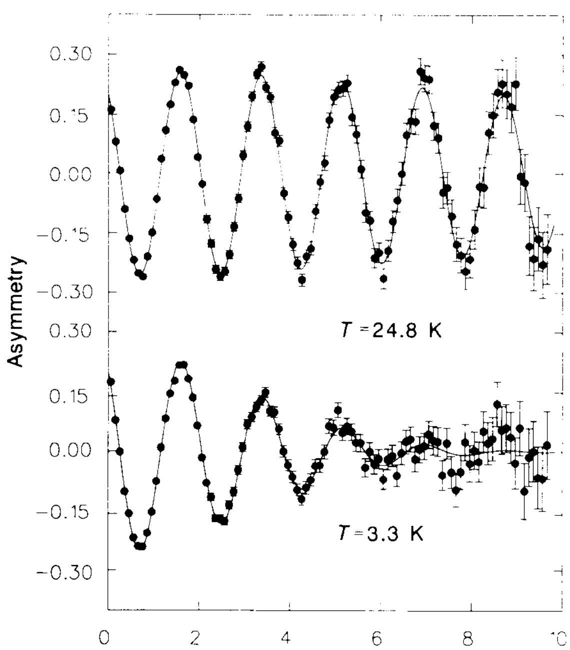

FIG. 1 Muon-spin-precession spectra in K_3C_{60} observed in a transverse external magnetic field $H_{ext} = 2$ kG after field cooling.

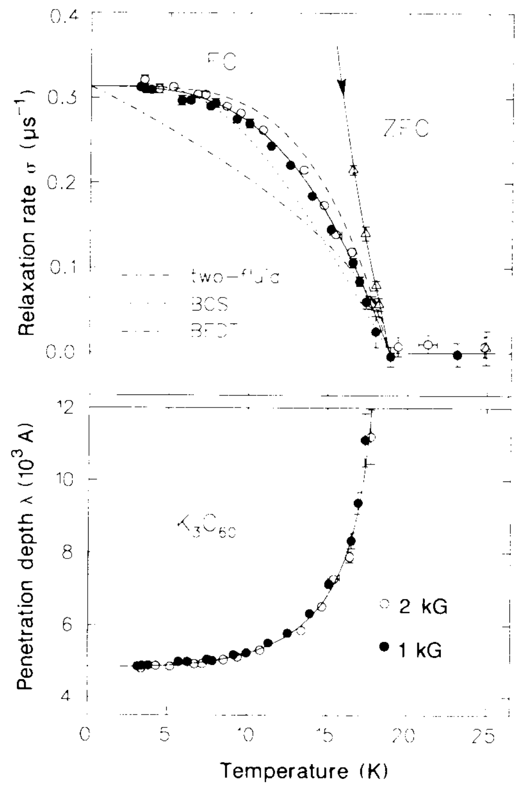

FIG. 2 *a*, Temperature dependence of the muon-spin-relaxation rate $\sigma(T)$ in K_3C_{60}. The solid line shows a fit to $\sigma(T) = [1-(T/T_c)^{3.2}]$ with $T_c = 18.9$ K. Also shown are curves expected for the two-fluid model, the BCS weak-coupling model and a recent μSR result in the BEDT system after normalizing by T_c. *b*, The magnetic field penetration depth λ in K_3C_{60} derived from $\sigma \propto \lambda^{-2}$.

ductors. This result indicates that K_3C_{60} has an isotropic energy gap without anomalous zeros: the system is most likely to be an s-wave superconductor.

This feature is common to the high-T_c cuprate, bismuthate (BKBO), Chevrel phase (see refs 6–10), and many other superconductors. For comparison, we show a curve of $\sigma(T)$ observed in (BEDT-TTF)$_2$Cu(NCS)$_2$ in a recent μSR study[10,15] in Fig. 2*a*. This curve has a linear variation in T at low temperatures, characteristic of anisotropic superconductors with line nodes in the energy gap[10,15]. The present results for $\sigma(T)$ in K_3C_{60} show a distinctly different temperature dependence with saturation at low temperatures, thus demonstrating isotropic pairing.

In general, the penetration depth λ is given as a function of n_s, m^*, ξ and the mean free path l as

$$\frac{1}{\lambda^2}=\frac{4\pi n_s e^2}{m^* c^2}\times\frac{1}{1+\xi/l}.$$

For systems close to the clean limit, $\xi/l\to 0$, the second term essentially becomes unity, and one expects a simple relation $\sigma\propto\lambda^{-2}\propto n_s/m^*$. Estimates of ξ from H_{c2} measurements and l from quantum oscillation and/or a.c.-conductivity studies indicate that the cuprate, organic BEDT, UPt_3 and some other systems lie close to the clean limit with $\xi/l\leq 0.3$. For K_3C_{60}, $\xi=26$ Å was obtained[5] from $H_{c2}\approx 50T$, while no reliable estimates are currently available for l. In view of the extremely short coherence length, here we assume that K_3C_{60} also lies close to the clean limit. With this assumption, we obtain the ground-state value $n_s/(m^*/m_e)\approx 1.2\times 10^{20}\ \mathrm{cm}^{-3}$. In a plot of T_c against $\sigma(T\to 0)$ comparing μSR results from different compounds[6,7], the present results from K_3C_{60} give a point for this system lying very close to the linear relation found for the cuprates, organic BEDT and some other systems. This implies that the ratio between T_c and $\sigma\propto n_s/m^*$ is roughly the same for these superconductors.

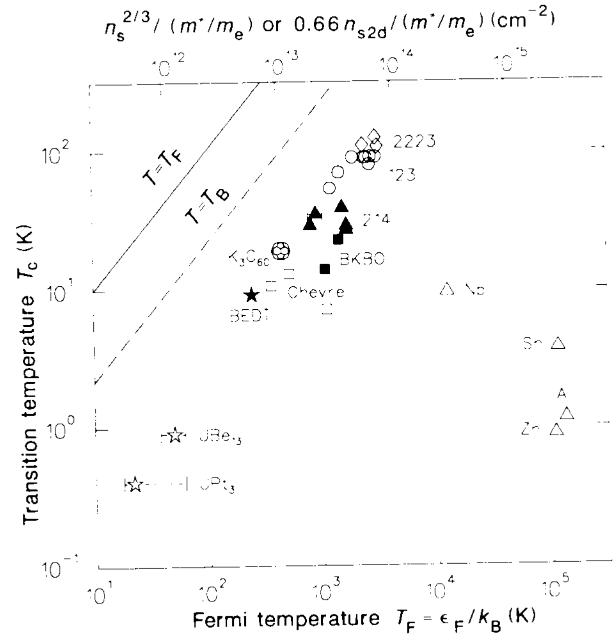

FIG. 3 A plot of T_c against the Fermi temperature T_f derived from our penetration depth measurements in K_3C_{60} (soccer-ball symbol) and various other superconductors (ref. 7 and refs therein). Open diamonds (2223) denote $Bi_2Sr_2(Ca,Pb)_2Cu_3O_{10}$ and cuprate compounds with similar structures: open circles (123) denote $YBa_2Cu_3O_y$ with $y=6.67$–7.0 and $Y_{0.7}Ca_{0.3}Ba_2Cu_3O_7$; filled triangles (214) denote $La_{2-x}Sr_xCuO_4$ with $x=0.1$–0.21; filled squares (BKBO) denote $Ba_{1-x}K_xBiO_3$ with $x=0.4$–0.5; open squares (Chevrel) denote $PbMo_6S_8$ and other nonmagnetic Chevrel-phase compounds. The broken line corresponds to the Bose–Einstein condensation temperature T_B for an ideal three-dimensional boson gas with a boson density $\frac{1}{2}n_s$ and mass $2m^*$. n_s is defined in the text; n_{s2d} is a two-dimensional number density (see ref. 7 for details).

The Fermi temperature T_F can be derived from $\sigma\propto n_s/m^*$. In three-dimensional systems, σ has to be combined with one other parameter containing either n_s or m^*, or their combination, to calculate $T_F\propto n_s^{2/3}/m^*$. As described in ref. 7, the most convenient way is to use the Sommerfeld constant $\gamma\propto n_s^{1/3}m^*$, to obtain $T_F\propto n_s^{2/3}/m^*\propto\sigma^{3/4}\gamma^{-1/4}$. In K_3C_{60}, a strong contribution from low-energy vibrational modes in the specific heat prevents a reliable determination of γ. Here we use the coherence length $\xi=(\hbar v_F)/(\Delta_G\pi)$, assuming the energy gap $\Delta_G=1.76k_BT_c$, which gives the Fermi velocity $v_F=3.6\times 10^6\ \mathrm{cm\ s}^{-1}$. Combining $\sigma\propto n_s/m^*$ and $v_F\propto n_s^{1/3}/m^*$, we obtain $T_F=470$ K assuming the formula

$$k_BT_F=(\hbar^2/2)(3\pi^2)^{2/3}n_s^{2/3}/m^*\propto\sigma^{1/2}v_F^{1/2}$$

for a noninteracting free-electron gas. The value of T_F thus calculated does not necessarily correspond to the Fermi temperature in detailed band-structure calculations, but does represent a characteristic energy scale for the superconducting carriers in the system. The same combination of parameters also yields $m^*=11m_e$ and $n_s=1.4\times 10^{21}\ \mathrm{cm}^{-3}$, which is close to the carrier density expected for one charge carrier per C_{60} molecule. Thus, K_3C_{60} has a narrow band with a low carrier density.

In Fig. 3 we compare the results from K_3C_{60} with those from other systems[7] in a plot of T_c against T_F. No corrections are made for ξ/l in calculating T_F: these would shift points towards the right-hand side on the horizontal axis, but would not alter the essential features. K_3C_{60} lies along the linear trend common to the 'exotic' superconductors defined in ref. 7. The ratio $T_c/T_F=1/25$ in K_3C_{60} is fairly large and close to those in high-T_c cuprate and two-dimensional organic BEDT superconductors, although these systems have different crystal and electronic structures and dimensionalities. Implications of the linear trend have been discussed in ref. 7.

Finally, we report on flux-pinning properties of K_3C_{60}. In zero-field cooling (ZFC) measurements with H_{ext}, flux lines cannot reach an equilibrium configuration if they are pinned in the process of moving from the edge to the inside of the specimen. This broadens the local field and produces a corresponding increase in σ. Therefore, the flux-pinning temperature T_p can be determined by μSR as the temperature below which the ZFC values of σ deviate from the FC values. As shown in Fig. 2*a*, values of $\sigma(T)$ measured in ZFC are larger than those in FC even at temperatures very close to T_c indicating $T_p/T_c\geq 0.95$ at $H_{ext}=2$ kG in K_3C_{60}. Earlier studies[16,17] suggest a tendency for systems with larger two-dimensional anisotropy, such as the Bi2212 cuprate or (BEDT-TTF)$_2$Cu[N(CN)$_2$]Br (ref. 15), to have lower values of T_p/T_c. The present finding in the isotropic K_3C_{60} is consistent with this empirical trend. □

Received 1 July; accepted 23 July 1991.

1. Hebard, A. F. *et al. Nature* **350**, 600–601 (1991).
2. Rosseinsky, M. J. *et al. Phys. Rev. Lett.* **66**, 2830–2832 (1991).
3. Holczer, K. *et al. Science* **252**, 1154–1157 (1991).
4. Stephens, P. W. *et al. Nature* **351**, 632–634 (1991).
5. Holczer, K. *et al. Phys. Rev. Lett.* **67**, 271–274 (1991).
6. Uemura, Y. J. *et al. Phys. Rev. Lett.* **62**, 2317–2320 (1989).
7. Uemura, Y. J. *et al. Phys. Rev. Lett.* **66**, 2665–2668 (1991).
8. Keller, H. *IBM J. Res. Dev.* **33**, 314–322 (1989).
9. Uemura, Y. J. *et al. Physica* **C162–164**, 857–860 (1989).
10. Uemura, Y. J. *Physica* **B169**, 99–106 (1991).
11. Sparn, G. *et al. Science* **252** (in the press).
12. Pincus, P., Gossard, A. C., Jaccarino, V. & Wernick, J. H. *Phys. Lett.* **13**, 31–33 (1964).
13. Brandt, E. H. *Phys. Rev.* **B37**, 2349–2352 (1988).
14. Rickayzen, G. *Theory of Superconductivity* (Wiley, New York, 1965).
15. Le, L. P. *et al. High-Temperature Superconductor-M²S III Conf.; Physica C* (in the press).
16. Pümpin, B. *et al. Z. Phys.* **B72**, 175 (1988).
17. Sternlieb, B. J. *et al. Physica* **C162–164**, 679–680 (1989).

ACKNOWLEDGEMENTS. S. J. Anz and F. Ettl produced and separated the molecular carbon samples used here. This work is supported by the David and Lucile Packard Foundation (Y.J.U., R.L.W. and R.B.K.), the NSF, the Office of Naval Research (F.D.) and the Natural Science and Engineering Research Council of Canada.